

Stabilized photorefractive running holograms, with arbitrarily selected phase shift, for material characterization

Ivan de Oliveira,¹ Agnaldo A. Freschi,² Igor Fier,³
and Jaime Frejlich^{4,*}

¹Faculdade de Tecnologia/ UNICAMP, Limeira-SP, Brazil

²Universidade Federal do ABC/UFABC, Santo André-SP, Brazil

³Dept. de Física, Instituto de Geociências e Ciências Exatas/ UNESP, Rio Claro-SP, Brazil

⁴Instituto de Física/ UNICAMP, Campinas-SP, Brazil

*frejlich@ifi.unicamp.br

Abstract: We report on the recording of stabilized running holograms in photorefractive materials with arbitrarily selected phase shift φ between the transmitted and diffracted beams propagating along the same direction behind the photorefractive crystal. The dependence of the diffraction efficiency and of the hologram speed on φ , in such stabilized holograms, can be easily measured and used for material characterization. In this communication we applied for the first time this technique for studying and characterizing hole-electron competition in a nominally undoped titanosillenite crystal sample.

© 2012 Optical Society of America

OCIS codes: (160.5320) Photorefractive materials; (050.7330) Volume gratings.

References and links

1. L. Solymar, D. J. Webb, and A. Grunnet-Jepsen, *The Physics and Applications of Photorefractive Materials* (Clarendon Press, Oxford, 1996).
2. S. I. Stepanov, V. V. Kulikov, and M. P. Petrov, "Running holograms in photorefractive Bi₁₂TiO₂₀ crystals," *Opt. Commun.* **44**, 19–23 (1982).
3. B. I. Sturman, M. Mann, J. Otten, and K. H. Ringhofer, "Space-charge waves and their parametric excitation," *J. Opt. Soc. Am. B* **10**, 1919–1932 (1993).
4. B. I. Sturman, M. Mann, and K. H. Ringhofer, "Instability of the resonance enhancement of moving photorefractive gratings," *Opt. Lett.* **18**, 702–704 (1993).
5. B. I. Sturman, E. V. Podivilov, A. I. Chemykh, K. H. Ringhofer, V. P. Kamenov, H. C. Pedersen, and P. M. Johansen, "Instability of the resonance excitation of space-charge waves in sillenite crystals," *J. Opt. Soc. Am. B* **16**, 556–564 (1999).
6. M. Bryushinin, "Interaction of running gratings of the space charge and conductivity in photorefractive Bi₁₂Si(Ti)O₂₀ crystals," *Appl. Phys. B* **79**, 851–856 (2004).
7. I. de Oliveira and J. Frejlich, "Photorefractive running hologram for materials characterization," *J. Opt. Soc. Am. B* **18**, 291–297 (2001).
8. M. Bryushinin, V. Kulikov, and I. Sokolov, "Combined excitation of running space charge and conductivity gratings in photorefractive crystals," *Phys. Rev. B* **71**, 165208 (2005).
9. I. de Oliveira and J. Frejlich, "Detection of resonance space-charge wave peaks for holes and electrons in photorefractive crystals," *J. Opt. Soc. Am. B* **26**, 1298–1302 (2007).
10. A. A. Kamshilin, J. Frejlich, and L. Cescato, "Photorefractive Crystals for the Stabilization of the Holographic Setup," *Appl. Opt.* **25**, 2375–2381 (1986).
11. J. Frejlich, L. Cescato, and G. F. Mendes, "Analysis of an active stabilization system for a holographic setup," *Appl. Opt.* **27**, 1967–1976 (1988).
12. J. Frejlich, P. M. Garcia, and L. Cescato, "Adaptive Fringe-Locked Running Hologram in Photorefractive Crystals," *Opt. Lett.* **14**, 1210–1212 (1989).

13. I. de Oliveira and J. Frejlich, "Gain and stability in photorefractive two-wave mixing," *Phys. Rev. A* **64**, 033806 (2001).
14. F. P. Strohkendl, J. M. C. Jonathan, and R. W. Hellwarth, "Hole-electron competition in photorefractive gratings," *Opt. Lett.* **11**, 312–314 (1986).
15. J. Frejlich, "Fringe-Locked Running Hologram and Multiple Photoactive Species in $\text{Bi}_{12}\text{TiO}_{20}$," *J. Appl. Phys.* **68**, 3104–3109 (1990).
16. R. Montenegro, A. Shumelyuk, R. Kumamoto, J. F. Carvalho, R. C. Santana, and J. Frejlich, "Vanadium-doped photorefractive titanosillenite crystal," *Appl. Phys. B* **95**, 475–482 (2009).
17. E. Shamonina, K. H. Ringhofer, P. M. Garcia, A. A. Freschi, and J. Frejlich, "Shape-asymmetry of the diffraction efficiency in $\text{Bi}_{12}\text{TiO}_{20}$ crystals: the simultaneous influence of absorption and higher harmonics," *Opt. Commun.* **141**, 132–136 (1997).
18. J. Frejlich, A. A. Freschi, P. M. Garcia, E. Shamonina, V. Y. Gayvoronsky, and K. H. Ringhofer, "Feedback-controlled running holograms in strongly absorbing photorefractive materials," *J. Opt. Soc. Am. B* **17**, 1517–1521 (2000).
19. M. Barbosa, L. Mosquera, and J. Frejlich, "Speed and diffraction efficiency in feedback-controlled running holograms for photorefractive crystal characterization," *Appl. Phys. B* **72**, 717–721 (2001).
20. A. Salazar, H. Lorduy, R. Montenegro, and J. Frejlich, "An improved procedure for fringe-locked photorefractive running hologram data processing," *J. Opt. A: Pure Appl. Opt.* **11**, 045201 (2009).
21. A. A. Freschi and J. Frejlich, "Adjustable phase control in stabilized interferometry," *Opt. Lett.* **20**, 635–637 (1995).
22. A. A. Freschi, P. M. Garcia, and J. Frejlich, "Phase-controlled photorefractive running holograms," *Opt. Commun.* **143**, 257–260 (1997).
23. R. Montenegro, A. A. Freschi, and J. Frejlich, "Photorefractive two-wave mixing phase coupling measurement in self-stabilized recording regime," *J. Opt. A: Pure Appl. Opt.* **10**, 104006 (2008).
24. G. C. Valley, "Erase rates in photorefractive materials with two photoactive species," *Appl. Opt.* **22**, 3160–3164 (1983).
25. M. Carrascosa and F. Agullo-Lopez, "Erasure of holographic gratings in photorefractive materials with two active species," *Appl. Opt.* **27**, 2851–2857 (1988).
26. K. Buse, "Light-induced charge transport processes in photorefractive crystals I: Models and experimental methods," *Appl. Phys. B* **64**, 273–291 (1997).
27. I. de Oliveira, R. Montenegro, and J. Frejlich, "Hole-electron electrical coupling in photorefractive materials," *Appl. Phys. Lett.* **95**, 241908 (2009).
28. J. Frejlich, *Photorefractive Materials: Fundamental Concepts, Holographic Recording, and Materials Characterization* (Wiley-Interscience, New York, 2006).
29. V. Jerez, I. de Oliveira, and J. Frejlich, "Optical recording mechanisms in undoped titanosillenite crystals," *J. Appl. Phys.* **109**, 024901 (2011).

1. Introduction

The generation of running holograms in photorefractive materials were thoroughly studied since long, for analysing the recording process itself [1–6] and for material characterization [6–9].

The use of self-stabilization techniques for holographic recording [10, 11] in conditions where a nonstationary hologram arises was shown [12] to produce so called fringe-locked running holograms that were later used for analysing the recording process [13] and for material and hole-electron competition [14] characterization in photorefractives [15, 16]. The effect of bulk light absorption on the dielectric relaxation and its effect on running hologram recording was demonstrated [17] and taken into account for improving the mathematical model for feedback-operated running hologram recording [18]. Such feedback controlled running holograms under strong light absorption were used for material characterization too [19, 20]. The use of a feedback setup enabling stabilized recording with arbitrarily selected holographic phase shift ϕ (the phase shift between the transmitted and diffracted beams along the same direction behind the crystal) was shown [21] to produce photorefractive running holograms with controlled speed and diffraction efficiency. In this way almost environmental perturbation-free (stabilized) running holograms with known and fixed phase shift values could be produced [22] and used for photorefractive materials characterization [23]. Still very important is the fact that the latter technique allows accurately computing ϕ directly from the zeroing of the error

signal, which is a combination of the first and second temporal harmonics produced by the piezoelectric-driven phase modulation in the setup, without requiring the knowledge of several setup parameters like the amplification of the lock-in amplifiers and the response of the piezoelectric [7] that may be quite nonlinear indeed.

In this paper we take advantage of such stabilized running holograms, with arbitrarily selected φ , for characterizing nominally undoped photorefractive titanosillenite crystals. The diffraction efficiency (η) and the running hologram speed v (or detuning $\Omega = Kv$, K being the hologram wave vector value) are measured as a function of the arbitrarily selected φ , for characterizing some parameters of the electron as well as of the hole photoactive centers in the samples.

2. Theory

The present theoretical development is based on the two-photoactive centers model [24–26], one center (donors) for electrons and the other (acceptors) for holes. The strong light absorption effect on the response time is also considered. The space-charge field evolution based on electron and on hole charge carriers are respectively described by the couple of equations [9]:

$$\tau_{sc1} \frac{\partial E_{sc1}(t)}{\partial t} + E_{sc1}(t) + \kappa_{12} E_{sc2}(t) + m E_{eff1} e^{-i\Omega t} = 0 \quad (1)$$

$$\tau_{sc2} \frac{\partial E_{sc2}(t)}{\partial t} + E_{sc2}(t) + \kappa_{21} E_{sc1}(t) + m E_{eff2} e^{-i\Omega t} = 0 \quad (2)$$

with the parameters

$$E_{effj} \equiv \frac{E_0 + iE_{Dj}}{1 + K^2 l_{sj}^2 - iKl_{Ej}} \quad (3)$$

$$\frac{1}{\tau_{scj}} = \frac{1}{\tau_{Mj}} \frac{1 + K^2 l_{sj}^2 - iKl_{Ej}}{1 + K^2 L_{Dj}^2 - iKL_{Ej}} = \omega_{Rj} + i\omega_{Ij} \quad (4)$$

$$\tau_{Mj} = \varepsilon \varepsilon_0 / (q \mu_j \mathcal{N}_j) \quad (5)$$

$$\kappa_{12} = \frac{\xi_1}{1 + K^2 l_{s1}^2 - iKl_{E1}} \quad \kappa_{21} = \frac{\xi_2}{1 + K^2 l_{s2}^2 - iKl_{E2}} \quad (6)$$

$$E_{D1} = Kk_B T / q \quad E_{D2} = -Kk_B T / q \quad (7)$$

$$KL_{Ej} = K^2 L_{Dj}^2 E_0 / E_{Dj} \quad (8)$$

$$Kl_{Ej} = E_0 / E_{qj} \quad (9)$$

where $\iota \equiv \sqrt{-1}$, the subindex $j = 1$ is always for electrons and $j = 2$ for holes, with E_0 being the externally applied electric field, k_B the Boltzmann constant, T the absolute temperature, ε_0 the permittivity of vacuum, ε the dielectric constant and q the absolute value of the electron electric charge. The density of free charge carriers and their mobility in the extended states (Conduction or Valence Bands) are \mathcal{N}_j and μ_j , respectively, and E_{qj} is the limit value of the space-charge field. The phenomenological parameter ξ_j accounts for the effect of the Debye length (l_{sj}) on the electric coupling when the interacting charges are spatially separated, as proposed elsewhere [27]. The solution of Eqs. (1) and (2) is:

$$E_{sc}(t) = E_{sc1}(t) + E_{sc2}(t) = -m E_{sc}^{st} e^{-i\Omega t} \quad (10)$$

where E_{sc}^{st} assumes the simplified expression:

$$E_{sc}^{st} = E_{eff1} \frac{\omega_{R1} + i\omega_{I1}}{\omega_{R1} + i\omega_{I1} - i\Omega} + E_{eff2} \frac{\omega_{R2} + i\omega_{I2}}{\omega_{R2} + i\omega_{I2} - i\Omega} \quad (11)$$

for $\xi_{1,2}$ [27] being small enough to assume that $\kappa_{12} \approx \kappa_{21} \approx 0$.

The diffraction efficiency η and the phase shift φ , accounting on self-diffraction and bulk absorption effects, can be written as [28]:

$$\eta = \frac{2\beta^2}{1+\beta^2} \frac{\cosh(\bar{\Gamma}d/2) - \cos(\bar{\gamma}d/2)}{\beta^2 e^{-\bar{\Gamma}d/2} + e^{\bar{\Gamma}d/2}} \quad (12)$$

$$\tan \varphi = -\frac{\sin(\bar{\gamma}d/2)}{\frac{1-\beta^2}{1+\beta^2} [\cosh(\bar{\Gamma}d/2) - \cos(\bar{\gamma}d/2)] + \sinh(\bar{\Gamma}d/2)} \quad (13)$$

with β^2 being the pump-to-signal beam intensity ratio and

$$\bar{\Gamma}d \equiv \int_0^d (\Gamma) dz \quad \Gamma \equiv \frac{2\pi n^3 r_{\text{eff}}}{\lambda} \Im\{E_{\text{sc}}^{\text{st}}\} \quad (14)$$

$$\bar{\gamma}d \equiv \int_0^d (\gamma) dz \quad \gamma \equiv \frac{2\pi n^3 r_{\text{eff}}}{\lambda} \Re\{E_{\text{sc}}^{\text{st}}\} \quad (15)$$

Here $\Re\{\}$ and $\Im\{\}$ represent the real and the imaginary parts respectively and z is the coordinate along the crystal thickness. The quantities $\bar{\Gamma}$ and $\bar{\gamma}$ are here introduced in order to take account on the effect of the bulk absorption α on the τ_{Mj} , as reported elsewhere [18]. In fact, because of the relatively large value of α , $\tau_{Mj} = \tau_{Mj}(z)$ does depend on the coordinate z along the crystal thickness:

$$\tau_{Mj}(z) = \tau_{Mj}(0) e^{\alpha z} \quad \tau_{Mj}(0) = \frac{\varepsilon \varepsilon_0 (k_B T / q) h \nu}{q L_D^2 \alpha I(0) \Phi_j} \quad (16)$$

with Φ_j being the quantum efficiency for charge carriers (electrons or holes) photogeneration with light of photonic energy $h\nu$. Consequently ω_{Rj} and ω_{Ij} do also depend on z as well as the derived $E_{\text{sc}}^{\text{st}}$, Γ and γ quantities. It was already shown elsewhere [7, 18], that using the spatial averages $\bar{\Gamma}$ and $\bar{\gamma}$ instead of the plain Γ and γ , in the expressions for η and $\tan \varphi$, the effect of the bulk absorption on these quantities are effectively taken into account.

3. Experiment and results

Holographic gratings were recorded using a $\lambda = 514.5$ nm laser light on a $d = 2.35$ mm thick nominally undoped photorefractive titanosillenite crystal $\text{Bi}_{12}\text{TiO}_{20}$ (labelled BTO-J13) produced by Prof. J.F. Carvalho at the Institute of Physics of the Universidade Federal de Goiás (UFG), Goiânia-GO, Brazil. The crystal is used in a transverse configuration with symmetrically incident recording beams, with the electric field E_0 applied along the [110]-axis, parallel to the hologram wavevector \vec{K} , and the [001]-axis perpendicular to the incidence plane. The bulk absorption of the crystal at the operating wavelength was $\alpha \approx 10.50 \text{ cm}^{-1}$. The recording was carried out using self-stabilization with an arbitrarily selected phase shift φ as described elsewhere [21, 22].

The experimental procedure is as follows: An external electric field E_0 is applied and a phase shift φ is fixed at a chosen value by means of the stabilization feedback loop so that the latter makes the recording pattern of fringes to run at a speed v ($\Omega = Kv$) in order to allow recording a photorefractive hologram with the chosen parameters E_0 and φ . The diffraction efficiency of this running hologram is measured in these conditions and plotted (\bullet) in Fig. 1 as a function of φ , for a constant E_0 . The detuning $\Omega = Kv$ as a function of φ is also measured and plotted in Fig. 2. From the two figures above, η is plotted as a function of Ω in Fig. 3. The continuous curve in Fig. 3 is the best theoretical fitting of Eq. (12) to the experimental data, with the

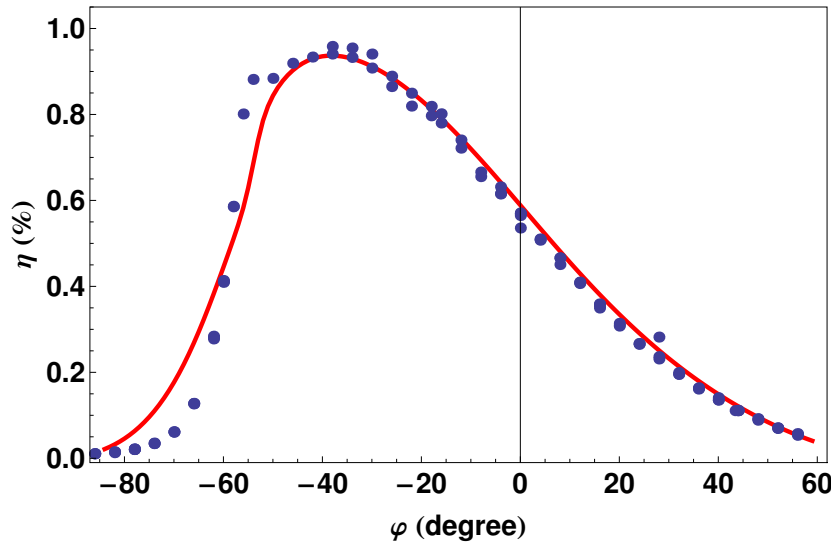


Fig. 1. Diffraction efficiency η data (\bullet) plotted as a function of φ for $E_0 = 5.6$ kV/cm and $K = 9.9 \mu\text{m}^{-1}$, $\beta^2 = 57$ with total incident irradiance $I_0 = 25.4$ mW/cm², together with a theoretical curve with the parameters reported in the first row in Table 1.

resulting material parameters displayed in the 3rd row of Table 1. Because of the low K -value involved in this experiment, the best fitted parameters L_{D1} and l_{s1} (with $K^2 L_{D1}^2 \ll 1$ and $K^2 l_{s1}^2 \ll 1$) are not much reliable. Nevertheless this set of parameters are useful as a starting point to find out theoretical curves (continuous lines) fairly well adjusting the experimental data in Figs. 1 and 2, where $K^2 L_{Dj}^2$ and $K^2 l_{sj}^2$ are not anymore negligibly small because a larger K value is used. The resulting parameters from the continuous curves in Figs. 1 and 2 are displayed in the 1st and 2nd rows, respectively, in Table 1.

Table 1. Material Parameters

DATA	E_0 (kV/cm)	K (μm^{-1})	Φ_1	Φ_2	L_{D1} (nm)	L_{D2} (nm)	l_{s1} (nm)	l_{s2} (nm)
Fig. 1	5.6	9.9	0.64	0.011	163	485	50	287
Fig. 2	5.6	9.9	0.40	0.011	170	485	50	287
Fig. 3	6.5	2.1	0.64	0.011	163	485	125	287

Parameters in 3rd column were obtained by direct data fitting.

The results in Table 1 show that the most reliable parameters found out for electrons and holes are: $\Phi_1 = 0.40 - 0.64$ and $\Phi_2 \approx 0.011$, $L_{D1} = 163 - 170$ nm and $L_{D2} \approx 485$ nm, $l_{s1} \approx 50$ nm and $l_{s2} \approx 287$ nm. These parameters, at least for electrons, are not far from those ($\Phi_1 = 0.33$, $L_{D1} = 160$ nm and $l_{s1} = 38$ nm) already published [20] for the same sample. The parameters for holes, on the other hand, are roughly coherent with their expected lower concentration and experimentally verified reduced participation in the recording process.

The hologram recorded on this undoped titanosillenite crystal was experimentally shown (as already reported before [29]) to be easily and rapidly erased using $\lambda = 1200$ nm light from a LED (light emitting diode) having a photonic energy slightly above 1 eV. The latter

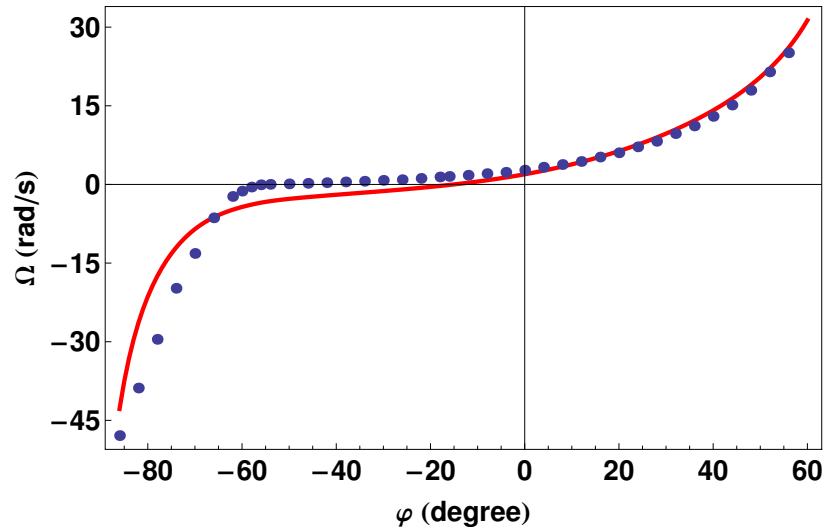


Fig. 2. Detuning $\Omega = Kv$ data (\bullet) plotted as a function of φ for $E_0 = 5.6$ kV/cm and $K = 9.9 \mu\text{m}^{-1}$, $\beta^2 = 57$ with total incident irradiance $I_0 = 25.4$ mW/cm², together with a theoretical curve with the parameters reported in the second row in Table 1.

is close to the energy gap between the top of the Valence Band and the Fermi level, where the main photoactive centers are localized and where it is expected that the space-charge field-based hologram be recorded. As optical recording is known to occur mainly by electrons, that need to be excited to the bottom of the Conduction Band (2.2 eV above the Fermi level), we should conclude that holes (to be excited to the top of the Valence Band 1 eV below the Fermi level) are responsible for 1200 nm light erasure. This result indicates that holes are actually participating (although in a much lower proportion than electrons) in optical recording (and erasure) in undoped sillenites, in agreement with our detection and measurement of material parameters of holes in the present running hologram experiments.

4. Conclusions

The present paper shows that running hologram experiments produced under carefully controlled conditions may be useful for characterizing photorefractive materials and even detect minority (more than $I_{s2}^2/I_{s1}^2 \approx 30$ -fold lower concentration) charge carriers (holes in this case) even if a relatively large number of unknown parameters are involved. In the present case, the combined use of large and small values for K helped to optimize the parameters to be found out from experimental data fitting: from low K values we may overlook some of the diffusion and Debye lengths so as to find out reliable values for the remaining parameters. Electrons and holes being electrically uncoupled, as formulated in Eq. (11), was experimentally verified and enabled the independent determination of parameters for both type of charge carriers here. From data displayed in Table 1 for electrons and for holes it becomes evident that parameters for electrons are much more relevant for curve shaping than are those for holes, so that the latter remain rather unchanged while the former vary sensibly from one experiment to the other. This is probably due to the fact that electrons are majority carriers and therefore have far larger influence in determining the adjustment of theoretical curves.

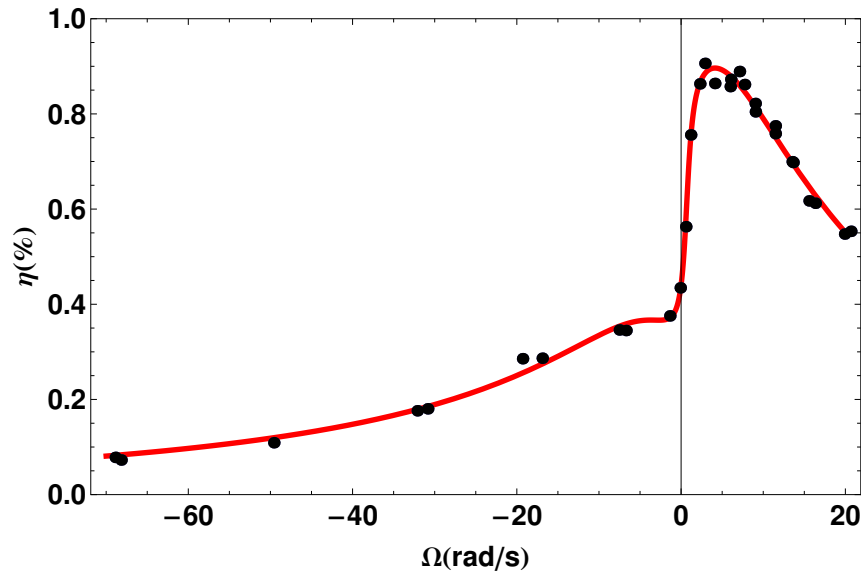


Fig. 3. Diffraction efficiency η data (\bullet) plotted as a function of detuning $\Omega = K\nu$ for $E_0 = 6.5$ kV/cm and $K = 2.1 \mu\text{m}^{-1}$, $\beta^2 = 29$, with total incident irradiance $I_0 = 17.3$ mW/cm², together with the theoretical best fitting curve with the parameters as reported in the third row in Table 1.

Acknowledgments

We acknowledge partial financial support from the Conselho de Desenvolvimento Científico e Tecnológico (CNPq), Fundação de Amparo à Pesquisa do Estado de São Paulo (FAPESP), FUNCAMP-Fundo de Apoio ao Ensino, Pesquisa e Extensão (FAEPEX-PAPIDC) and Coordenação de Aperfeiçoamento de Pessoal de Nível Superior (CAPES) all from Brazil. We are grateful to Prof. Dr. Jesiel F. Carvalho from the Institute of Physics of the Federal University of Goiás-GO, Brazil, for the excellent photorefractive crystal sample used in this research.